Obesity due to Steroid Receptor Coactivator-1 deficiency is associated with endocrine and metabolic abnormalities

Tessa M Cacciottolo, Elana Henning, Julia M Keogh, Pierre Bel Lassen, Katherine Lawler, Rebecca Bounds, Rachel Ahmed, Aliki Perdikari, Edson Mendes de Oliveira, Miriam Smith, et al.

Obesity due to Steroid Receptor Coactivator-1 deficiency is associated with endocrine and metabolic abnormalities

Tessa M. Cacciottolo, M.D., Ph.D.[1], Elana Henning, B.Soc.Sc.[1], Julia M. Keogh, B.Sc.[1], Pierre Bel Lassen, M.D.[2], Katherine Lawler, Ph.D.[1], Rebecca Bounds, Ph.D.[1], Rachel Ahmed B.Sc.[1], Aliki Perdikari, Ph.D.[1], Edson Mendes de Oliveira, Ph.D.[1], Miriam Smith, Ph.D.[1], Edmund M. Godfrey, M.A., BM. BCh.[3], Elspeth Johnson, B.Sc.[4], Leanne Hodson, Ph.D. [4], Karine Clément, M.D., Ph.D.[2], Agatha A. van der Klaauw, M.D., Ph.D.[1]*, I. Sadaf Farooqi, M.B. Ch.B., Ph.D.[1]*

[1]University of Cambridge Metabolic Research Laboratories and NIHR Cambridge Biomedical Research Centre, Wellcome-MRC Institute of Metabolic Science, Box 289, Addenbrooke's Hospital, Cambridge CB2 0QQ, UK; [2]Sorbonne Université, INSERM, Nutrition and obesities : systemic approaches (NutriOmics) research group and Assistance Publique hôpitaux de Paris, Nutrition department, Pitié-Salpêtrière Hospital, Paris, France; [3]Department of Radiology, Addenbrooke's Hospital, Cambridge CB2 0QQ, UK; [4]Oxford Centre for Diabetes, Endocrinology and Metabolism, University of Oxford, Churchill Hospital and National Institute for Health Research Oxford Biomedical Research Centre, Oxford University Hospitals Foundation Trust, UK. Co-corresponding authors*. Corresponding authors' contact information: Agatha A. van der Klaauw, av330@medschl.cam.ac.uk; I. Sadaf Farooqi, isf20@cam.ac.uk. Reprint requests should be addressed to Sadaf Farooqi: isf20@cam.ac.uk

Grants or Fellowships supporting the paper: This study was supported by funding from Wellcome (207462/Z/17/Z to ISF, 099038/Z/12/Z to AAvdK), the NIHR Cambridge Biomedical Research Centre, Botnar Fondation and the Bernard Wolfe Health Neuroscience Endowment (to ISF). TMC was supported by a Philip Greenwood Clinical Research Fellowship and a Wellcome Trust Research Training Fellowship (203513/Z/16/Z). LH is a British Heart Foundation Senior Research Fellow in Basic Science (FS/15/56/31645). KC is supported by the Fondation pour la Recherche Médicale and the French National Agency of research (ANR-Captor project) and Direction générale de la Santé (DGOS, Clinical Research Contract CRC-Fibrota). Clinical studies were performed on the IMS Translational Research Facility; histology was performed by the IMS Histology core; both are funded by Wellcome (208363/Z/17/Z). The views expressed are those of the author(s) and not necessarily those of the NHS, the NIHR, or the Department of Health and Social Care.

Disclosure summary: The authors have no conflicts of interest relevant to this article to disclose.

Abstract

Context: Genetic variants affecting the nuclear hormone receptor coactivator Steroid Receptor Coactivator, *SRC-1,* have been identified in people with severe obesity and impair melanocortin signaling in cells and mice. As a result, obese patients with SRC-1 deficiency are being treated with a Melanocortin 4 receptor agonist in clinical trials.

Objective: Here, our aim was to comprehensively describe and characterise the clinical phenotype of *SRC-1* variant carriers to facilitate diagnosis and clinical management.

Design: In genetic studies of 2,462 people with severe obesity, we identified 23 rare heterozygous variants in *SRC-1*. We studied 29 adults and 18 children who were *SRC-1* variant carriers and performed measurements of metabolic and endocrine function, liver imaging and adipose tissue biopsies. Findings in adult *SRC-1* variant carriers were compared to 30 age and BMI-matched controls.

Results: The clinical spectrum of *SRC-1* variant carriers included increased food intake in children, normal basal metabolic rate, multiple fractures with minimal trauma (40%), persistent diarrhea, partial thyroid hormone resistance and menorrhagia. Compared to age, sex and BMI matched controls, adult *SRC-1* variant carriers had more severe adipose tissue fibrosis (46.2% v 7.1% respectively, P=0.03) and a suggestion of increased liver fibrosis (5/13 cases versus 2/13 in controls, odds ratio 3.4), although this was not statistically significant.

Conclusions: *SRC-1* variant carriers exhibit hyperphagia in childhood, severe obesity and clinical features of partial hormone resistance. The presence of adipose tissue fibrosis and hepatic fibrosis in young patients suggests that close monitoring for the early development of obesity-associated metabolic complications is warranted.

Keywords: SRC-1, nuclear hormone receptors, obesity, hormone resistance.

Introduction

Single gene disorders which disrupt the development and/or function of the hypothalamic leptin-melanocortin pathway cause hyperphagia (increased food intake), neuroendocrine abnormalities, impaired sympathetic tone and weight gain from early childhood (1). Establishing a genetic diagnosis is helpful for patients and families and clinical guidelines recommend genetic testing as part of the diagnostic evaluation of people with severe obesity that begins in childhood (2). Genetic findings increasingly impact on clinical care as a number of therapies are now licensed in the US and Europe for the chronic weight management of people with genetic obesity syndromes (3,4).

In a previous exome sequencing study of 2,548 European ancestry patients with severe, early-onset obesity (mean Body Mass Index (BMI) standard deviation score>3; age of onset <10 years) (5), we reported rare heterozygous variants in the gene encoding Steroid Receptor Coactivator-1 (SRC-1) (6). SRC-1 is a widely expressed coactivator which modulates the activity of nuclear hormone receptors and other transcription factors; targeted deletion of *SRC-1* causes obesity in mice (7). We showed that in the hypothalamus, SRC-1 interacts with phosphorylated STAT3 (Signal Transducer and Activator of Transcription-3) to potentiate leptin-mediated transcription of Pro-opiomelanocortin (POMC) (6); POMC-derived melanocortin peptides signal through the Melanocortin-4 receptor (MC4R) to reduce food intake (Figure 1a). In mice, deletion of *SRC-1* in Pomc neurons decreased *Pomc* expression and increased food intake leading to obesity (6). Human obesity-associated variants in *SRC-1* impaired leptin-mediated Pomc reporter activity in cells, predominantly through a dominant negative effect. We established a causal link between rare human variants and obesity by characterising a knock-in mouse model of a human loss-of-function (LOF) *SRC-1* variant which exhibited increased food intake and weight gain (6). As a result of these studies, patients with severe obesity and rare *SRC-1* variants are now being recruited into Phase 2 clinical trials of Setmelanotide, a MC4R agonist, licensed for the chronic weight management of POMC and Leptin receptor

deficiency (3,8,9). As patients with SRC-1 deficiency are increasingly being identified by genetic screening in obesity clinics, and as their identification has potential implications for therapy, the aim of this study is to describe the clinical spectrum seen in patients with rare variants in *SRC-1* to facilitate diagnosis and clinical management.

In this study, we identified additional carriers of rare variants (global minor allele frequency (MAF) <0.1% across all populations) in *SRC-1* using exome sequencing and targeted resequencing of patients with severe obesity (methods as reported previously (5,10)). As well as developing obesity, *SRC-1* knock-out mice exhibit resistance to thyroid hormone (11) and partial resistance to oestrogen, progesterone and testosterone (12), manifesting as decreased growth and development of the uterus, ovaries, mammary glands and testes (12) and loss of trabecular bone mass (13). Furthermore, SRC-1 interacts with Farnesoid-X receptor (FXR) and Liver X Receptor (LXR), regulators of *de novo* lipogenesis (DNL) (14) and with PGC-1α to mediate the activity of PPAR-γ, a master regulator of adipogenesis and thermogenesis in mice (7). Here we explored clinical features in a cohort of 47 *SRC-1* variant carriers who consented to clinical studies, focussing on the metabolic and endocrine phenotypes that may arise from impaired nuclear hormone receptor mediated gene transcription.

Patients and Methods

Patients and Study Design

We studied patients with severe obesity (Body Mass Index (weight in kg/height in metres^2; BMI) standard deviation score>3) of early-onset (<10 years of age) recruited to the Genetics of Obesity Study (GOOS) cohort (www.goos.org.uk). These studies were approved by the Cambridge Local Research Ethics Committee (03/103, 03/104, 18/EE/0032) and conducted in accordance with the principles of the Declaration of Helsinki. Each participant or their legal guardian (for children under

16 years of age) provided written, informed consent and minors provided verbal or written consent. Exome sequencing and targeted resequencing were performed as previously described (5); all variants were verified by Sanger sequencing.

We performed a series of studies to describe the clinical features of *SRC-1* variant carriers. We compared data from adult variant carriers with that obtained on obese volunteers recruited by advertisement who were carefully matched for age, sex and BMI and in whom variants in *SRC-1* were excluded by Sanger sequencing. Those with co-morbidities (type 2 diabetes, auto-immune hypo- and hyperthyroidism and/or taking levothyroxine treatment) and concomitant medications which affect body weight and/or metabolism were excluded from clinical studies. Some measurements were not performed on all eligible cases and controls for a variety of reasons (weight limit for DXA and/or MRI, challenging vascular access, medications); numbers studied are indicated for each measurement. Eighteen children with variants in *SRC-1* were compared to 11 age-matched controls. Whilst adult controls were matched for BMI, paediatric controls were not, as equally severely obese children often have other genetic conditions.

Adipose tissue samples (Paris obesity cohort) were obtained from people with severe obesity prospectively recruited to the Prospective Bariatric Surgery Cohort of the Nutrition Department at Pitié-Salpêtrière Hospital, Paris, France between 2014 and 2018. They are part of several studies registered on ClinicalTrials.gov (P050318, NCT01655017, NCT01454232). Informed consent was obtained to perform paired omental and subcutaneous surgical adipose tissue biopsies obtained during bariatric surgery. In the surgical department in Paris, patients are asked to have a stabilized weight prior to bariatric surgery and do not routinely consume a restrictive diet pre-operatively in contrast to clinical practice at other centres. Details of adipose tissue handling have been reported previously (15).

Anthropometry, body composition and liver imaging

Weight and height were measured barefoot in light clothing. Dual X-ray absorptiometry (DXA) (DPX software; Lunar Corp) was used to determine body composition, bone mineral content and density (whole body ~~and at the hip and lumbar spine~~). Subcutaneous and visceral fat mass were quantified in a subset of cases and controls by Magnetic Resonance Imaging (MRI) at the level of L1 and analysed using OsiriX Lite software (Pixmeo, Switzerland). In a subset of 13 *SRC-1* variant carriers and 15 controls, MRI scans were carried out on a wide bore 1.5T whole body system (GE Medical Systems, Waukesha, WI) and included localiser images, T2w fat saturated images, proton density fat fraction (PDFF) and magnetic resonance elastography (MRE). Participants were fasted for four hours prior to the procedure, and were positioned in the supine position with an acoustic driver positioned superficial to the liver. Liver volume: T2w images were used to draw regions of interest (ROIs) around the liver perimeter on consecutive slices and volume computed using OsiriX Lite (Pixmeo, Switzerland). Images for Proton Density Fat Fraction (PDFF) were acquired using a gradient echo sequence with a low flip angle which were then analysed using the validated IDEAL-IQ software (GE Healthcare) to generate an unbiased quantitative measure of percentage fat fraction. Magnetic Resonance Elastography (MRE) was used to quantify hepatic fibrosis (>2.9 kPa correlates with significant hepatic fibrosis on histology and a METAVIR score of ≥F2 (16)). MRE images were acquired using a phase contrast gradient echo sequence. Where participants were unable to have MRI (weight ≥230 kg, abdominal girth ≥70 cm), acoustic radiation frequency impulse (ARFI) elastography or mechanical impulse elastography (Fibroscan) was performed. ARFI was performed using Canon shearwave elastography by a trained radiologist on an Aplio 500 (version 2 software) or Aplio i800. Mechanical impulse elastography was performed with Fibroscan (Echosens, France) using the XL probe. Results were accepted if they met recognised reliability criteria (IQR/median < 0.3) (17). Operators were blinded to genotype. Two participants were unable to have an MRI scan (weight ≥230 kg, abdominal girth ≥70 cm), as such acoustic radiation frequency imaging (ARFI) or transient elastography (TE) was performed.

Metabolic measurements and autonomic function

Ad libitum energy intake was assessed using an 18MJ meal of known macronutrient content (50% carbohydrate, 30% fat, 20% protein) administered after an overnight fast; energy intake was expressed per kilogram of lean body mass as measured by DXA to allow comparison between individuals of different body weights and compositions. Basal metabolic rate and respiratory quotient were determined by indirect calorimetry after a 10 hour overnight fast using an open circuit, ventilated, canopy measurement system (Europa Gas Exchange Monitor; NutrEn Technology). After adjustment for body composition, basal metabolic rate was compared to predicted metabolic rate based on standard age and sex specific equations. Blood pressure was measured in the rested fasted state using automated wrist (OMRON Healthcare) monitors. We used a DINAMAP automated brachial monitor with the Dura large adult cuff (GE Healthcare) in three people whose wrist circumference precluded use of this device. Heart rate was measured using a digital portable heart rate monitor (ActiHeart, Cambridge Technologies). Heart rate data collected using the portable heart rate monitor was exported to MS Excel 2010 via Actiheart software (Version 4.0.116, CamNtech Ltd., Cambridge, UK). Overnight readings were taken between 0000 h and 0500 h when each participant was asleep; awake readings were taken during a 30 minute window directly after the participant had woken up. Heart rate variability was analysed with Kubios HRV Premium (version 3.4.1, Kubios, Kuopio, Finland) by two researchers who were blinded to genotype.

Glucose homeostasis and Endocrine function

Blood samples were obtained in the fasting state and analysed for lipids, thyrotropin stimulating hormone (TSH), free T4, free T3, luteinising hormone, follicle stimulating hormone, estradiol, testosterone and cortisol with the use of standard assays. In addition, an oral glucose tolerance test examining the glucose and insulin response to 75 g oral glucose load over 180 minutes was

performed in 15 adult variant carriers and 14 controls who did not have a diagnosis of type 2 diabetes.

Adipose tissue biopsies

In 13 cases and 14 age, sex and BMI-matched controls who consented to the procedure, subcutaneous adipose tissue biopsies were obtained from the left iliac fossa, using a non-diathermy surgical biopsy method, under local anaesthesia (1% lidocaine with 1:200,000 adrenaline). A 2-3 cm skin incision was made, skin flaps were raised on either side of the incision and the superficial fascia incised. Approximately 2 g of adipose tissue was excised and washed in phosphate-buffered saline. Separate sections (4 μm) of subcutaneous adipose tissue were stained with haematoxylin and eosin (H & E) and Picosirius red (PSR) and scanned using the Axio Scan.Z1 slide scanner (Zeiss, Cambridge, UK) into whole digital images. In order to evaluate adipocyte morphology and measure adipocyte surface area, H&E stained slides were processed using HALO image analysis software (Indica Labs, Albuquerque, USA). All adipocytes in the section were included in the analysis, adipocyte surface area was measured using the inbuilt Vacuole v2.2 algorithm. Scoring of anonymised samples from cases with *SRC-1* variants and controls (UK and Paris groups) was performed by the same observer (PBL). Values were used to generate a frequency distribution with a bin width of 500 μm. In order to quantify adipose tissue fibrosis, PSR stained slides were assessed using the FAT score (18) by an experienced observer (PBL), blinded to the identity of the samples. Severe adipose tissue fibrosis was defined as FAT score ≥ 2 as previously described (18).

De novo lipogenesis

We measured *de novo* lipogenesis (DNL) in 14 cases and 16 age, sex and BMI matched controls. Fasting blood samples were collected at 2000 h, and a priming dose of deuterium-labelled water (3 ml x 0.5 x body weight (kg) for females; 3 ml x 0.6 x body weight (kg) males) was made up to 200 ml with tap water and provided in two equal portions at 2000 h and 2200 h. *Ad libitum* deuterated water (4.5 ml/L) was provided overnight; no food was permitted. A blood sample was collected at 0800 h the following morning. Participants were then provided with breakfast comprising 50% of energy requirements (60% carbohydrate, 30% fat, 10% protein), a further portion of deuterated water at 1000 hrs and a final blood sample collected at 1200 h.

Total plasma lipids were extracted using chloroform-methanol and triglyceride (TG) separated by solid-phase extraction (19). Fatty acid methyl esters were prepared using methanolic sulphuric acid and fatty acid relative abundance (mol %) was determined by gas chromatography (19). Fasting and postprandial hepatic DNL was assessed based on the incorporation of deuterium from $^{2}H_2O$ in plasma water (Finnigan GasBench-II, ThermoFisher Scientific, UK) into plasma TAG palmitate using gas chromatography-mass spectrometry (GC-MS), monitoring ions with mass-to-charge ratios of 270 (M+0) and 271 (M+1) (20). Background isotopic enrichment in plasma water was measured in a fasting blood sample taken before subjects consumed deuterated water. Plasma metabolites (3-hydroxybutyrate, triglyceride, non-esterified fatty acids (NEFA)) were analysed enzymatically (ILab 650 clinical chemistry; Werfen, Warrington, UK).

Statistical analysis

Statistical analysis was performed using R and GraphPad prism v9 statistical packages. All datasets were checked for normality of distribution using the Shapiro-Wilk, Kolmogorov-Smirnov tests, and equality of variance using the F test. Datasets with normal distributions and equal variance were compared using an unpaired t test and nonparametric data was compared using the Mann-Whitney

U test. Where multiple comparisons were performed, the Holm-Sidak correction for multiple comparisons was used to compute the adjusted P value. Statistical tests are two-tailed unless otherwise stated and significance of an individual test was declared at $p < 0.05$.

Results

Identification of rare variants in *SRC-1*

In this study, we performed exome sequencing and targeted resequencing of 2,462 people with severe obesity and identified 23 rare heterozygous variants in *SRC-1* (Figure 1b); a number of variants were found in multiple unrelated individuals and some were present in publicly available exomes (Table 1). In a previous study, we identified 15 variants in 16 unrelated individuals amongst 2,548 people with severe obesity studied using the same methods (6) and showed they caused a loss-of-function (LOF) in cells using a POMC reporter assay (Table 1). Whilst we did not perform functional studies of the 23 variants identified in this new study, the variants identified here affect the domain known to interact with STAT3 and the domain that interacts with nuclear hormone receptors (NHRs; Nuclear receptor interacting domain, NRID) (Figure 1b). We have previously shown that variants affecting these domains can cause a LOF (6).

We performed family co-segregation studies and found that rare variants in *SRC-1* did not consistently co-segregate with severe obesity in a Mendelian manner (Figure 2). This was true even for variants shown to cause a clear loss of function in cells previously (6). We conclude that rare *SRC-1* variants are not fully penetrant but rather may interact with other genetic and/or environmental factors to modulate the phenotype. These findings align with those reported for other obesity-associated genes (*MRAP2, KSR2, PHIP* (10,21,22)) where rare heterozygous variants are associated with obesity but not always causative, in contrast to the classical monogenic obesity syndromes which follow an autosomal recessive (*LEP, LEPR, POMC, PCSK1*) or dominant (*MC4R, SIM1, GNAS*)

mode of inheritance (1).

Clinical features seen in a cohort of patients with SRC-1 deficiency

We invited all probands with rare variants in *SRC-1* and their affected family members to take part in clinical studies. Twenty-nine adults and 18 children (under 18 years) with rare variants in *SRC-1* consented to take part (Figure 3a). Twenty-nine adult *SRC-1* variant carriers were studied using a core phenotyping protocol (Table 2); mean (+/- SD) age 31.4 ± 2.1 years (range 18.2 to 49.8 years); their data was compared to 30 controls (mean (+/- SD) age 30.9 ± 1.7 years (range 19.0 to 48.4 years, P=0.94). The mean BMI of the adult *SRC-1* variant carriers was 41.8 ± 13.3 kg/m² (23.3 to 74.9 kg/m²) and controls 43.2 ± 12.7 kg/m^2 (26.8 to 85.2 kg/m^2, P=0.62). A subset of these individuals, 15 SRC-1 cases and 16 controls, consented to take part in a metabolic sub-study which involved liver imaging, adipose tissue biopsies and stable isotope studies of *de novo* lipogenesis (Figure 3a and Table 2).

A high proportion (40%; n=19) of *SRC-1* variant carriers had a history of fractures in response to minor injuries in contrast to patients with other genetic obesity syndromes (1) (Figure 3b). Whole body bone mineral density was comparable in cases and controls (BMD Z score 0.6 ± 0.2 vs 0.7 ± 0.2, respectively). Whilst none of the *SRC-1* variant carriers had thyroid function tests suggestive of resistance to thyroid hormone (high TSH/ high FT4, Table 3), interestingly, thyroxine treatment for autoimmune hypothyroidism of the women carrying the L1376P and A715T variants was complicated by failure to adequately suppress TSH, despite high dose (> 200 µg) levothyroxine, unless free thyroxine levels were above 25 pmol/l (normal range 10-19.8 pmol/l). We carefully reviewed compliance with thyroxine therapy. Notably, there were no features of malabsorption or bowel disease at colonoscopy in the patient carrying L1376P SRC-1.

Menstrual irregularities are common in women with obesity. We found that 13% (2/15) of women (age 16-50 years) with *SRC-1* variants had a history of polycystic ovarian syndrome (with hyperandrogenism and hirsutism); this was comparable to severely obese women with MC4R deficiency (9%; 2/22) of comparable BMI. In addition, eight out of 18 female *SRC-1* variant carriers older than 16 years old (44%) reported menorrhagia with persistent bleeding (Figure 3b). One female *SRC-1* variant carrier was diagnosed with complex atypical endometrial hyperplasia in her early 20s, which responded well to progestogen therapy. One female variant carrier of the L1376P variant had primary amenorrhoea. Women with *SRC-1* variants were more likely to be prescribed tranexamic acid for persistent bleeding 13.5 % (4/15) than women with MC4R deficiency (0 of 22) we have studied.

Four out of twelve adult male *SRC-1* variant carriers had low testosterone and gonadotropin levels consistent with hypogonadotropic hypogonadism (Figure 3b). Three out of these four variant carriers had signs of primary hypogonadism (undescended testis, reduced penile length). In comparison, 3 out of 8 male controls had low testosterone and gonatropin levels, consistent with secondary hypogonadotropic hypogonadism. None of the variant carriers had overt clinical signs or symptoms of mineralocorticoid or corticosteroid hormone resistance.

A number of *SRC-1* variant carriers had been diagnosed with hepatic fibrosis or cirrhosis at a young age (Figure 3b). Liver function tests were within the normal range in cases and controls (Table 3); liver volume determined by T2 weighted MRI (2126 ± 545 cm^3 in cases v 2388 ± 661 cm^3 in controls, P=0.29) and liver fat assessed using MRI-Proton Density Fat Fraction (MRI-PDFF) was comparable in cases and controls (7.1% vs 10.9% respectively, P=0.38). We found that 5 out of 13 (38%) adult *SRC-1* variant carriers had significant hepatic fibrosis compared to 2 out of 13 (15%) adult controls; odds ratio 3.4 (P=0.38). Fourteen *SRC-1* variant carriers (30%) reported frequent and/or persistent diarrhoea, described as pale, loose stools, typically after fatty food. There was no biochemical

evidence of macro or micronutrient malabsorption (Table 3). These features could be consistent with bile acid malabsorption; further studies will be required to test this.

Twelve *SRC-1* variant carriers (25%) had moderate to severe asthma requiring home nebulisers, frequent courses of oral corticosteroids and/or hospital admissions (Figure 3b). STAT3 is a major regulator of the differentiation and function of Th17 cells, a subset of $CD4^+$ T-cells implicated in inflammation in patients with severe asthma. Three variant carriers had pulmonary valve stenosis, a rare congenital abnormality (population prevalence 3/10,000 births). Further studies will be needed to explore the mechanisms underlying these observations.

Body fat distribution, energy intake and expenditure

Children demonstrated increased food intake at an 18 MJ *ad libitum* test meal compared to age-matched controls (Figure 3c); food intake was not increased in adults with *SRC-1* variants compared to controls (Figure 3d). In contrast to findings in SRC-1 deficient mice, there was no deficit in measured basal metabolic rate, which correlated tightly with that predicted by age, sex and body composition (R=0.6989, P=0.0013, Figure 3e). Heart rate and heart rate variability (markers of autonomic nervous system tone) were comparable between the groups (Table 3). We quantified the ratio of visceral (VAT) to subcutaneous (SAT) adipose tissue using Magnetic Resonance Imaging (MRI). VAT: SAT was comparable in *SRC-1* variant carriers and controls (1.49 ± 0.91 in cases v 1.27 ± 0.48 in controls, P=0.9).

Glucose and lipid homeostasis

Two out of 29 *SRC-1* variant carriers had a diagnosis of type 2 diabetes. Although SRC-1 has been implicated in hepatic glucose production (23), we did not find any differences in fasting glucose or insulin levels or in the area under the curve (AUC) during a 75 g oral glucose tolerance test (OGTT)

between *SRC-1* variant carriers and controls (Figure 4a and b, Table 3). Fasting lipid profiles were within the normal range in cases and controls (Table 3). We measured fasting and post-prandial *de novo* lipogenesis (DNL) using deuterated water. There was no difference between cases and controls in fasting hepatic DNL, expressed as percent or a concentration (Table 3). With meal consumption, DNL increased in both groups to a similar extent (Table 3). We found no difference in fasting plasma concentrations of 3-hydroxybutyrate (3OHB), a marker of hepatic fatty acid oxidation, between cases and controls (Table 3). As expected, there was a significant decrease in plasma 3OHB concentrations post-prandially in both groups (Table 3). Fasting NEFA concentrations were not significantly different between cases and controls (Table 3). Whilst post-prandial NEFA concentrations decreased in both groups, this decline was attenuated in cases vs controls (191.7 ± 15.6 µmol/l vs 137.1 ± 18.7 µmol/l, respectively, P = 0.02) which may suggest impaired insulin sensitivity of the adipose tissue.

Adipose tissue morphology and fibrosis

Both omental and subcutaneous adipose tissue can undergo fibrosis in people with obesity (24,25). Increased adipose tissue fibrosis is associated with inflammation (26) and may lead to decreased tissue plasticity and thus a failure to expand fat mass with sustained weight gain (27,28). In addition, adipose tissue fibrosis is associated with reduced weight loss following bariatric surgery in people with severe obesity (18,29). *SRC-1* variant carriers had a higher proportion of smaller adipocytes (500 μm^2) compared to controls (21.7 ± 4.3 % in cases vs 19.6 ± 6.0 % in controls, adjusted P=0.02). Further analysis of the tissue demonstrated marked fibrosis in biopsies taken from several cases (Figure 4c and d). The degree of fibrosis was assessed using a previously reported score (called the FAT score; (18)). A greater proportion of *SRC-1* variant carriers had severe fibrosis (FAT Score 2-3) compared to age, sex and BMI-matched controls (46.2% vs. 7.1%, P=0.03) (Figure 4e). There was no correlation between FAT score and BMI in either group. In addition, we compared our findings to

those from a cohort of 265 similarly obese patients (mean BMI +/- SD 46.3 ± 14.1 vs 46.6 ± 6.4 kg/m^2, P=0.93) attending for bariatric surgery in Paris, France (data on 183 of these patients was previously published (18)). The prevalence of severe fibrosis was comparable in both groups (46.2 % v 39.2 %, P=0.7), although the Paris control group was significantly older than the *SRC-1* variant carriers in our study (31.4 ± 12.1 vs 42.9 ± 12.1 years respectively, P<0.01) (Figure 4f).

Discussion

In this study, we describe the clinical features seen in people with severe obesity carrying rare variants in *SRC-1*. In keeping with findings in patients with other genetic disorders affecting the leptin-melanocortin pathway, *SRC-1* variant carriers experience hyperphagia in childhood, but have a normal basal metabolic rate and mild insulin resistance. These findings are consistent with previous findings showing that SRC-1 interacts with phosphorylated STAT3 to modulate leptin-mediated POMC transcription and with findings in a mouse model of a human LOF *SRC-1* variant (6).

We observed a very high prevalence of multiple fractures with minimal trauma in males and females starting from childhood, in contrast to findings in patients with other genetic obesity syndromes such as MC4R deficiency (30). SRC-1 plays an important role in the development and maintenance of bone density, primarily through its interaction with the estrogen receptor (ER) (31,32). The skeletal impact of *SRC-1* variants may also be mediated by resistance to the vitamin D receptor (VDR) and the TH receptor which function as heterodimers with retinoid X receptor (RXR). Whilst we did not observe a reduction in whole body bone mineral density in SRC-1 cases vs controls, it is important to note that deletion of *SRC-1* results in trabecular osteopenia in male and female mice (13). Trabecular bone accounts for only 20% of total bone mass in humans. Targeted spine, femur, femoral neck and distal radius DEXA scans and/or high resolution peripheral quantitative computed tomography or bone histology may be needed to investigate the impact of SRC-1 deficiency on bone architecture.

SRC-1 enhances thyroid hormone (TH) receptor mediated signaling (33). *SRC-1* knockout mice display resistance to TH (RTH) with a 2.5-fold elevation of TSH levels, despite a 50% increase in free TH levels (11). Whilst none of the *SRC-1* variant carriers in our study had overt classical RTH, treatment of concomitant autoimmune hypothyroidism was complicated by failure to suppress TSH in 2 variant carriers, despite high dose thyroxine. There was no suggestion of non- or intermittent compliance, and there were no features of malabsorptive disorders such as coeliac disease or bowel disease. Interestingly, the decline of TSH observed in mice treated with L-triiodothyronine is blunted in *SRC-1* knockout mice indicating that SRC-1 enhances the sensitivity by which TH downregulates TSH (11,34). Studies in larger cohorts of patients will be needed to establish whether partial thyroid hormone resistance, as seen in *SRC-1* knockout mice, is a feature in some people with *SRC-1* variants.

Multiple female *SRC-1* variant carriers reported severe menorrhagia which significantly impacted on quality of life. SRC-1 is expressed in the endometrium, its expression increases during menstruation in both the glandular epithelium and stroma where it may play a role in endometrial remodelling (35,36) which depends on the balance of estrogen and progesterone signaling (12,37). Interestingly, a truncated SRC-1 isoform has been implicated in the pathophysiology of endometriosis (38). The complex atypical endometrial hyperplasia of one of the *SRC-1* variant carriers did respond to progestogens, suggesting that any subtle defects in progesterone signaling due to *SRC-1* variants may be overcome by pharmacotherapy with progesterone.

Generally, increased adipose tissue mass is characterised by adipocyte hypertrophy followed by hyperplasia. In chronic obesity (as seen in the older patients studied in the Paris cohort), adipose tissue undergoes major remodelling, resulting in inflammation and fibrosis, which represents a physical constraint to adipose tissue expansion (39). Studies in rodents (40) (and insights from patients with lipodystrophy (41)) indicate that this reduction in adipose expandability promotes the deposition of excess lipid in liver and skeletal muscle leading to metabolic complications (42). Here,

glucose tolerance was comparable in cases and controls tightly matched for age and BMI. Whether increased adipose tissue fibrosis in young patients with *SRC-1* variants predisposes them to the early development of metabolic complications such as type 2 diabetes and fatty liver disease, is an important question that needs to be addressed in larger longitudinal studies. The observation that several patients have hepatic fibrosis (but not steatosis) is not readily explained and will require further investigation and long term monitoring.

Larger studies will be needed to test for genotype-phenotype correlations. While a common variant in the gene encoding SRC-1 (*NCOA1*) has been associated with reduced hip and lumbar bone mineral density in women receiving tamoxifen treatment (32), to date variants at this locus have not been associated with body mass index in genome wide association studies.

In conclusion, the clinical spectrum associated with *SRC-1* variants is characterised by hyperphagia in childhood and severe obesity and encompasses a range of other metabolic and endocrine features. The interpretation of these findings is challenging as several factors including the functional consequences of different *SRC-1* variants, the presence of residual SRC-1 activity in carriers of heterozygous variants and compensation by the closely related molecule SRC-2 (7), will contribute to phenotypic heterogeneity. Further functional characterisation of the *SRC-1* variants reported here will be needed to establish their pathogenicity. All are very rare, affect highly conserved residues and are located in domains in which we have previously identified loss-of-function variants. Nonetheless, as seen with the first clinical descriptions of functional variants affecting THR-α and –β and ER-α, these findings illustrate important aspects of physiology and pathophysiology. Human variants affecting SRC-1 will be useful molecular tools with which to dissect nuclear hormone receptor signaling and its regulation by coactivators and corepressors, studies which will provide insights into underlying disease mechanisms and ultimately inform the clinical investigation and management of patients.

Acknowledgments

We are indebted to the participants and their families for their participation and to the Physicians involved in the Genetics of Obesity Study (GOOS) (www.goos.org.uk). This study was supported by funding from Wellcome (207462/Z/17/Z to ISF, 099038/Z/12/Z to AAvdK), the NIHR Cambridge Biomedical Research Centre, the Botnar Foundation and the Bernard Wolfe Health Neuroscience Endowment (to ISF). Clinical studies were performed on the IMS Translational Research Facility, which is funded by Wellcome (208363/Z/17/Z). TMC was supported by a Philip Greenwood Clinical Research Fellowship and a Wellcome Trust Research Training Fellowship (203513/Z/16/Z). LH is a British Heart Foundation Senior Research Fellow in Basic Science (FS/15/56/31645). KC is supported by the Fondation pour la Recherche Médicale and the French National Agency of research (ANR-Captor project) and Direction générale de la Santé (DGOS, Clinical Research Contract CRC-Fibrota). The views expressed are those of the authors and not necessarily those of the NHS or the NIHR. The metabolic substudy data were collected and managed using REDcap electronic data capture tools hosted at the University of Cambridge. Figures 1 and 3 were prepared using Biorender.com.

Data Availability

Restrictions apply to the availability of some or all data generated or analyzed during this study to preserve patient confidentiality. The corresponding author will on request detail the restrictions and any conditions under which access to some data may be provided.

References

1. van der Klaauw AA, Farooqi IS. The hunger genes: pathways to obesity. *Cell*. 2015;161(1):119-132.
2. Styne DM, Arslanian SA, Connor EL, Farooqi IS, Murad MH, Silverstein JH, Yanovski JA. Pediatric Obesity-Assessment, Treatment, and Prevention: An Endocrine Society Clinical Practice Guideline. *J Clin Endocrinol Metab*. 2017;102(3):709-757.
3. Clement K, van den Akker E, Argente J, Bahm A, Chung WK, Connors H, De Waele K, Farooqi IS, Gonneau-Lejeune J, Gordon G, Kohlsdorf K, Poitou C, Puder L, Swain J, Stewart M, Yuan G, Wabitsch M, Kuhnen P, Setmelanotide P, Investigators LPT. Efficacy and safety of setmelanotide, an MC4R agonist, in individuals with severe obesity due to LEPR or POMC deficiency: single-arm, open-label, multicentre, phase 3 trials. *The lancet Diabetes & endocrinology*. 2020;8(12):960-970.
4. Farooqi IS, Jebb SA, Langmack G, Lawrence E, Cheetham CH, Prentice AM, Hughes IA, McCamish MA, O'Rahilly S. Effects of recombinant leptin therapy in a child with congenital leptin deficiency. *N Engl J Med*. 1999;341(12):879-884.
5. Hendricks AE, Bochukova EG, Marenne G, Keogh JM, Atanassova N, Bounds R, Wheeler E, Mistry V, Henning E, Korner A, Muddyman D, McCarthy S, Hinney A, Hebebrand J, Scott RA, Langenberg C, Wareham NJ, Surendran P, Howson JM, Butterworth AS, Danesh J, Nordestgaard BG, Nielsen SF, Afzal S, Papadia S, Ashford S, Garg S, Millhauser GL, Palomino RI, Kwasniewska A, Tachmazidou I, O'Rahilly S, Zeggini E, Barroso I, Farooqi IS. Rare Variant Analysis of Human and Rodent Obesity Genes in Individuals with Severe Childhood Obesity. *Scientific reports*. 2017;7(1):4394.

6. Yang Y, van der Klaauw AA, Zhu L, Cacciottolo TM, He Y, Stadler LKJ, Wang C, Xu P, Saito K, Hinton A, Jr., Yan X, Keogh JM, Henning E, Banton MC, Hendricks AE, Bochukova EG, Mistry V, Lawler KL, Liao L, Xu J, O'Rahilly S, Tong Q, Consortium UK, Ines B, O'Malley BW, Farooqi IS, Xu Y. Steroid receptor coactivator-1 modulates the function of Pomc neurons and energy homeostasis. *Nature communications*. 2019;10(1):1718.

7. Picard F, Gehin M, Annicotte J, Rocchi S, Champy MF, O'Malley BW, Chambon P, Auwerx J. SRC-1 and TIF2 control energy balance between white and brown adipose tissues. *Cell*. 2002;111(7):931-941.

8. Kuhnen P, Clement K, Wiegand S, Blankenstein O, Gottesdiener K, Martini LL, Mai K, Blume-Peytavi U, Gruters A, Krude H. Proopiomelanocortin Deficiency Treated with a Melanocortin-4 Receptor Agonist. *N Engl J Med*. 2016;375(3):240-246.

9. Clement K, Biebermann H, Farooqi IS, Van der Ploeg L, Wolters B, Poitou C, Puder L, Fiedorek F, Gottesdiener K, Kleinau G, Heyder N, Scheerer P, Blume-Peytavi U, Jahnke I, Sharma S, Mokrosinski J, Wiegand S, Muller A, Weiss K, Mai K, Spranger J, Gruters A, Blankenstein O, Krude H, Kuhnen P. MC4R agonism promotes durable weight loss in patients with leptin receptor deficiency. *Nat Med*. 2018;24(5):551-555.

10. Marenne G, Hendricks AE, Perdikari A, Bounds R, Payne F, Keogh JM, Lelliott CJ, Henning E, Pathan S, Ashford S, Bochukova EG, Mistry V, Daly A, Hayward C, Interval UKKC, Wareham NJ, O'Rahilly S, Langenberg C, Wheeler E, Zeggini E, Farooqi IS, Barroso I. Exome Sequencing Identifies Genes and Gene Sets Contributing to Severe Childhood Obesity, Linking PHIP Variants to Repressed POMC Transcription. *Cell Metab*. 2020;31(6):1107-1119 e1112.

11. Weiss RE, Xu J, Ning G, Pohlenz J, O'Malley BW, Refetoff S. Mice deficient in the steroid receptor co-activator 1 (SRC-1) are resistant to thyroid hormone. *The EMBO journal*. 1999;18(7):1900-1904.

12. Xu J, Qiu Y, DeMayo FJ, Tsai SY, Tsai MJ, O'Malley BW. Partial hormone resistance in mice with disruption of the steroid receptor coactivator-1 (SRC-1) gene. *Science*. 1998;279(5358):1922-1925.

13. Modder UI, Sanyal A, Xu J, O'Malley BW, Spelsberg TC, Khosla S. The skeletal response to estrogen is impaired in female but not in male steroid receptor coactivator (SRC)-1 knock out mice. *Bone*. 2008;42(2):414-421.

14. Knebel B, Fahlbusch P, Dille M, Wahlers N, Hartwig S, Jacob S, Kettel U, Schiller M, Herebian D, Koellmer C, Lehr S, Muller-Wieland D, Kotzka J. Fatty Liver Due to Increased de novo Lipogenesis: Alterations in the Hepatic Peroxisomal Proteome. *Front Cell Dev Biol*. 2019;7:248.

15. Rouault C, Marcelin G, Adriouch S, Rose C, Genser L, Ambrosini M, Bichet JC, Zhang Y, Marquet F, Aron-Wisnewsky J, Poitou C, Andre S, Derumeaux G, Guerre-Millo M, Clement K. Senescence-associated beta-galactosidase in subcutaneous adipose tissue associates with altered glycaemic status and truncal fat in severe obesity. *Diabetologia*. 2021;64(1):240-254.

16. Guglielmo FF, Venkatesh SK, Mitchell DG. Liver MR Elastography Technique and Image Interpretation: Pearls and Pitfalls. *Radiographics*. 2019;39(7):1983-2002.

17. Schwabl P, Bota S, Salzl P, Mandorfer M, Payer BA, Ferlitsch A, Stift J, Wrba F, Trauner M, Peck-Radosavljevic M, Reiberger T. New reliability criteria for transient elastography increase the number of accurate measurements for screening of

cirrhosis and portal hypertension. *Liver international : official journal of the International Association for the Study of the Liver*. 2015;35(2):381-390.

18. Bel Lassen P, Charlotte F, Liu Y, Bedossa P, Le Naour G, Tordjman J, Poitou C, Bouillot JL, Genser L, Zucker JD, Sokolovska N, Aron-Wisnewsky J, Clement K. The FAT Score, a Fibrosis Score of Adipose Tissue: Predicting Weight-Loss Outcome After Gastric Bypass. *J Clin Endocrinol Metab*. 2017;102(7):2443-2453.

19. Heath RB, Karpe F, Milne RW, Burdge GC, Wootton SA, Frayn KN. Selective partitioning of dietary fatty acids into the VLDL TG pool in the early postprandial period. *J Lipid Res*. 2003;44(11):2065-2072.

20. Semple RK, Sleigh A, Murgatroyd PR, Adams CA, Bluck L, Jackson S, Vottero A, Kanabar D, Charlton-Menys V, Durrington P, Soos MA, Carpenter TA, Lomas DJ, Cochran EK, Gorden P, O'Rahilly S, Savage DB. Postreceptor insulin resistance contributes to human dyslipidemia and hepatic steatosis. *J Clin Invest*. 2009;119(2):315-322.

21. Pearce LR, Atanassova N, Banton MC, Bottomley B, van der Klaauw AA, Revelli JP, Hendricks A, Keogh JM, Henning E, Doree D, Jeter-Jones S, Garg S, Bochukova EG, Bounds R, Ashford S, Gayton E, Hindmarsh PC, Shield JP, Crowne E, Barford D, Wareham NJ, O'Rahilly S, Murphy MP, Powell DR, Barroso I, Farooqi IS. KSR2 mutations are associated with obesity, insulin resistance, and impaired cellular fuel oxidation. *Cell*. 2013;155(4):765-777.

22. Asai M, Ramachandrappa S, Joachim M, Shen Y, Zhang R, Nuthalapati N, Ramanathan V, Strochlic DE, Ferket P, Linhart K, Ho C, Novoselova TV, Garg S, Ridderstrale M, Marcus C, Hirschhorn JN, Keogh JM, O'Rahilly S, Chan LF, Clark AJ, Farooqi IS,

Majzoub JA. Loss of function of the melanocortin 2 receptor accessory protein 2 is associated with mammalian obesity. *Science*. 2013;341(6143):275-278.

23. Louet JF, Chopra AR, Sagen JV, An J, York B, Tannour-Louet M, Saha PK, Stevens RD, Wenner BR, Ilkayeva OR, Bain JR, Zhou S, DeMayo F, Xu J, Newgard CB, O'Malley BW. The coactivator SRC-1 is an essential coordinator of hepatic glucose production. *Cell Metab*. 2010;12(6):606-618.

24. Pasarica M, Gowronska-Kozak B, Burk D, Remedios I, Hymel D, Gimble J, Ravussin E, Bray GA, Smith SR. Adipose tissue collagen VI in obesity. *J Clin Endocrinol Metab*. 2009;94(12):5155-5162.

25. Guglielmi V, Cardellini M, Cinti F, Corgosinho F, Cardolini I, D'Adamo M, Zingaretti MC, Bellia A, Lauro D, Gentileschi P, Federici M, Cinti S, Sbraccia P. Omental adipose tissue fibrosis and insulin resistance in severe obesity. *Nutr Diabetes*. 2015;5:e175.

26. Spencer M, Yao-Borengasser A, Unal R, Rasouli N, Gurley CM, Zhu B, Peterson CA, Kern PA. Adipose tissue macrophages in insulin-resistant subjects are associated with collagen VI and fibrosis and demonstrate alternative activation. *American journal of physiology Endocrinology and metabolism*. 2010;299(6):E1016-1027.

27. Chun TH, Hotary KB, Sabeh F, Saltiel AR, Allen ED, Weiss SJ. A pericellular collagenase directs the 3-dimensional development of white adipose tissue. *Cell*. 2006;125(3):577-591.

28. Khan T, Muise ES, Iyengar P, Wang ZV, Chandalia M, Abate N, Zhang BB, Bonaldo P, Chua S, Scherer PE. Metabolic dysregulation and adipose tissue fibrosis: role of collagen VI. *Molecular and cellular biology*. 2009;29(6):1575-1591.

29. Abdennour M, Reggio S, Le Naour G, Liu Y, Poitou C, Aron-Wisnewsky J, Charlotte F, Bouillot JL, Torcivia A, Sasso M, Miette V, Zucker JD, Bedossa P, Tordjman J, Clement

K. Association of adipose tissue and liver fibrosis with tissue stiffness in morbid obesity: links with diabetes and BMI loss after gastric bypass. *J Clin Endocrinol Metab*. 2014;99(3):898-907.

30. Farooqi IS, Keogh JM, Yeo GS, Lank EJ, Cheetham T, O'Rahilly S. Clinical spectrum of obesity and mutations in the melanocortin 4 receptor gene. *N Engl J Med*. 2003;348(12):1085-1095.

31. Yamada T, Kawano H, Sekine K, Matsumoto T, Fukuda T, Azuma Y, Itaka K, Chung UI, Chambon P, Nakamura K, Kato S, Kawaguchi H. SRC-1 is necessary for skeletal responses to sex hormones in both males and females. *Journal of bone and mineral research : the official journal of the American Society for Bone and Mineral Research*. 2004;19(9):1452-1461.

32. Hartmaier RJ, Richter AS, Gillihan RM, Sallit JZ, McGuire SE, Wang J, Lee AV, Osborne CK, O'Malley BW, Brown PH, Xu J, Skaar TC, Philips S, Rae JM, Azzouz F, Li L, Hayden J, Henry NL, Nguyen AT, Stearns V, Hayes DF, Flockhart DA, Oesterreich S. A SNP in steroid receptor coactivator-1 disrupts a GSK3beta phosphorylation site and is associated with altered tamoxifen response in bone. *Mol Endocrinol*. 2012;26(2):220-227.

33. Weiss RE, Gehin M, Xu J, Sadow PM, O'Malley BW, Chambon P, Refetoff S. Thyroid function in mice with compound heterozygous and homozygous disruptions of SRC-1 and TIF-2 coactivators: evidence for haploinsufficiency. *Endocrinology*. 2002;143(4):1554-1557.

34. Alonso M, Goodwin C, Liao X, Ortiga-Carvalho T, Machado DS, Wondisford FE, Refetoff S, Weiss RE. In vivo interaction of steroid receptor coactivator (SRC)-1 and the activation function-2 domain of the thyroid hormone receptor (TR) beta in

TRbeta E457A knock-in and SRC-1 knockout mice. *Endocrinology*. 2009;150(8):3927-3934.

35. Wieser F, Schneeberger C, Hudelist G, Singer C, Kurz C, Nagele F, Gruber C, Huber JC, Tschugguel W. Endometrial nuclear receptor co-factors SRC-1 and N-CoR are increased in human endometrium during menstruation. *Mol Hum Reprod*. 2002;8(7):644-650.

36. Shiozawa T, Shih HC, Miyamoto T, Feng YZ, Uchikawa J, Itoh K, Konishi I. Cyclic changes in the expression of steroid receptor coactivators and corepressors in the normal human endometrium. *J Clin Endocrinol Metab*. 2003;88(2):871-878.

37. Liu Z, Wong J, Tsai SY, Tsai MJ, O'Malley BW. Sequential recruitment of steroid receptor coactivator-1 (SRC-1) and p300 enhances progesterone receptor-dependent initiation and reinitiation of transcription from chromatin. *Proc Natl Acad Sci U S A*. 2001;98(22):12426-12431.

38. Han SJ, Hawkins SM, Begum K, Jung SY, Kovanci E, Qin J, Lydon JP, DeMayo FJ, O'Malley BW. A new isoform of steroid receptor coactivator-1 is crucial for pathogenic progression of endometriosis. *Nat Med*. 2012;18(7):1102-1111.

39. Marcelin G, Silveira ALM, Martins LB, Ferreira AV, Clement K. Deciphering the cellular interplays underlying obesity-induced adipose tissue fibrosis. *J Clin Invest*. 2019;129(10):4032-4040.

40. Shimomura I, Hammer RE, Ikemoto S, Brown MS, Goldstein JL. Leptin reverses insulin resistance and diabetes mellitus in mice with congenital lipodystrophy. *Nature*. 1999;401(6748):73-76.

41. Oral EA, Simha V, Ruiz E, Andewelt A, Premkumar A, Snell P, Wagner AJ, DePaoli AM, Reitman ML, Taylor SI, Gorden P, Garg A. Leptin-replacement therapy for lipodystrophy. *N Engl J Med*. 2002;346(8):570-578.

42. Alba DL, Farooq JA, Lin MYC, Schafer AL, Shepherd J, Koliwad SK. Subcutaneous Fat Fibrosis Links Obesity to Insulin Resistance in Chinese Americans. *J Clin Endocrinol Metab*. 2018;103(9):3194-3204.

Figure Legends

Figure 1: Obesity associated *SRC-1* variants. (a) SRC-1 modulates the leptin signaling pathway. Upon leptin binding, the leptin receptor (LEPR) phosphorylates JAK2, which in turn activates STAT3. Phosphorylated STAT3 (pSTAT3) dimerises and translocates to the nucleus where it binds to the *POMC* promoter. SRC-1 and other coactivators are recruited as part of a coactivator/corepressor complex and initiate transcription of the neuropeptide Pro-opiomelanocortin (POMC) which reduces food intake in the fed state. **(b)** Rare variants in *SRC-1* identified in individuals with severe early onset obesity. Variants previously reported (6) and found to cause a loss of function are denoted in black and located above the protein; newly identified variants are denoted in grey, below the protein. bHLH, basic helix-loop-helix; PAS, Per-Arnt-Sim (A and B) domains; NRID, nuclear receptor interacting domain; AD, activating domains 1 and 2; HAT, histone acetyl transferase domain.

Figure 2: Pedigrees of *SRC-1* Cases. Co-segregation of *SRC-1* variants is shown where male (squares) and female (circles) family members consented to genotyping. Heterozygous (filled) and wild-type (empty) *SRC-1* variant carriers indicated; some individuals were not available for genotyping (grey). Body mass index (BMI) (>25 kg/m^2 = overweight; >30 kg/m^2 = obesity) for adults and BMI standard deviation scores (BMI SDS) for children are shown where available. Arrow indicates the proband. Rhombus = unknown. * = Homozygous

Figure 3. Clinical features of *SRC-1* variant carriers. (a) 47 people with *SRC-1* variants consented to phenotypic studies. Twenty-nine adult *SRC-1* cases and 30 age, sex and BMI matched controls underwent core phenotyping studies; a subset of 15 *SRC-1* cases and 16 controls consented to additional metabolic phenotyping studies. Eighteen children with variants in *SRC-1* were compared to 11 age-matched controls. **(b)** Additional clinical features seen in *SRC-1* variant carriers; details of

age, sex and *SRC-1* variant are shown. **(c-d)** *Ad libitum* energy intake assessed using a 18MJ meal of known macronutrient content after an overnight fast in children **(c)** and adults **(d)**; food intake expressed per kilogram lean body mass measured by DXA. **(e)** Basal metabolic rate (BMR; megajoules, MJ/day) determined by indirect calorimetry after an overnight fast. Measured BMR was compared to BMR predicted by age and sex specific equations.

Figure 4. Glucose homeostasis and adipose tissue morphology in *SRC-1* variant carriers.

(a-b) Insulin and glucose levels during a 75g oral glucose tolerance test over 180 minutes in SRC-1 cases and controls. **(c-d)** Representative histology of subcutaneous adipose tissue biopsies taken from *SRC-1* variant carriers **(c)** and controls **(d),** stained for collagen, consistent with FAT score 3 and 0 respectively. Picosirius red staining, scale bar = 500 μm. **(e)** *SRC-1* variant carriers (cases) have a significantly higher proportion of severe adipose tissue fibrosis (FAT Score 2-3), compared to age, sex and BMI-matched controls. **(f)** Distribution of FAT score by age in *SRC-1* variant carriers (black circles), matched controls (open circles) and a large cohort of individuals with severe obesity undergoing bariatric surgery (grey circles, 'Paris obesity cohort').

Table 1. *SRC-1* variants identified in a cohort with severe obesity (GOOS)

SRC-1 Variant	Nucleotide Change	rs number	Number of probands with variant	gnoMAD Allele Frequencies							
				European (non-Finnish)	European (Finnish)	Latino/ Admixed American	East Asian	South Asian	African/ African American	Ashkenazi Jewish	Other
E210K	c.628G>A	rs573124083	1	3.517×10^{-5}	-	-	-	-	6.152×10^{-5}	-	-
T377N	c.1130C>A	rs139389349	7	1.787×10^{-4}	-	-	-	-	4.007×10^{-5}	-	1.387×10^{-4}
N378K	c.1134T>A	rs1015634733	1	4.408×10^{-5}	-	-	-	-	-	-	-
M381R	c.1142T>G	-	1	-	-	-	-	-	-	-	-
R385Q	c.1154G>A	rs776205465	1	7.751×10^{-6}	-	3.106×10^{-4}	-	3.267×10^{-5}	-	-	-
S389L	c.1166C>T	rs764983598	1	6.974×10^{-5}	-	2.822×10^{-5}	5.012×10^{-5}	-	-	-	-
H431R	c.1292A>G	rs202008308	5	4.725×10^{-4}	-	-	-	-	8.012×10^{-5}	-	-
G439R	c.1315G>A	rs371609618	1	8.796×10^{-6}	-	-	-	-	6.152×10^{-5}	-	-
Q448K	c.1342C>A	rs762401650	1	2.638×10^{-5}	-	-	-	-	-	-	-
Q463H	c.1389G>T	-	1	-	-	-	-	-	-	-	-
L541S	c.1622T>C	rs148155916	1	8.812×10^{-5}	-	-	-	-	-	-	-
N549S	c.1646A>G	rs541293975	3	3.102×10^{-5}	-	-	-	5.751×10^{-3}	4.096×10^{-5}	-	4.183×10^{-4}
S557T	c.1670G>C	rs772308327	1	5.428×10^{-5}	-	-	-	-	-	-	-

S565N	c.1694G>A	rs889784030	1	2.327×10^{-5}	-	-	-	3.266×10^{-5}	-	-	-
R572S	c.1716A>T	rs142018995	6	1.513×10^{-3}	1.990×10^{-4}	2.089×10^{-3}	-	-	3.249×10^{-4}	-	3.482×10^{-3}
Q597P	c.1790A>C	rs1459123790	1	1.556×10^{-5}	-	-	-	-	-	-	-
S603C	c.1807A>T	-	1	-	-	-	-	-	-	-	-
D710H	c.2128G>C	rs149214507	1	9.316×10^{-5}	-	5.647×10^{-5}	-	-	-	-	1.389×10^{-4}
A715T	c.2143G>A	rs752190418	1	8.816×10^{-6}	-	-	-	-	-	-	-
S738L	c.2213C>T	rs1486480744	1	1.762×10^{-5}	-	-	-	-	-	-	-
M791V	c.2371A>G	rs1034065067	1	-	-	5.855×10^{-5}	-	-	-	-	-
Q804R	c.2411A>G	rs758160275	1	-	-	1.844×10^{-5}	-	-	-	-	1.899×10^{-4}
A857T	c.2569G>A	rs145705009	4	7.685×10^{-4}	-	-	-	6.546×10^{-4}	8.013×10^{-5}	-	5.551×10^{-4}
T979P	c.2935A>C	-	1	-	-	-	-	-	-	-	-
M984T	c.2951T>C	rs151084207	1	8.795×10^{-6}	-	-	-	-	6.152×10^{-5}	-	-
P988S	c.2962C>T	rs763384268	1	8.794×10^{-6}	-	-	-	-	-	-	-
P1034L	c.3101C>T	-	1	-	-	-	-	-	-	-	-
T1083A	c.3247A>G	rs1271468598	1	-	-	-	-	-	-	-	-
N1142K	c.3426C>A	-	1	-	-	-	-	-	-	-	-
N1212K	c.3636C>G	rs1306789226	2	8.804×10^{-6}	-	-	-	-	-	-	-
Q1231E	c.3691C>G	-	1	-	-	-	-	-	-	-	-

V1238I	c.3712G>A	rs56099330	1	7.872×10^{-6}	-	8.930×10^{-5}	-	-	2.211×10^{-3}	-	1.418×10^{-4}
S1250I	c.3749G>T	rs754718198	1	8.798×10^{-6}	-	-	-	3.267×10^{-5}	-	-	-
P1257L	c.3770C>T	rs1219997834	1	8.794×10^{-6}	-	2.892×10^{-5}	-	3.267×10^{-5}	-	-	-
Y1277C	c.3830A>G	rs751254362	1	3.519×10^{-5}	-	-	-	-	-	-	-
T1326M	c.3977C>T	rs759588390	1	3.244×10^{-4}	-	-	-	-	-	-	-
N1332S	c.3995A>G	rs150066931	6	9.757×10^{-4}	1.194×10^{-4}	5.361×10^{-4}	-	2401×10^{-2}	4.008×10^{-5}	9.066×10^{-3}	4.016×10^{-3}
L1376P	c.4127T>C	rs201252444	1	5.42×10^{-5}	-	1.185×10^{-3}	-	-	-	9.643×10^{-5}	1.385×10^{-3}

Variant numbering based on Ensembl transcript ID ENST00000406961. Allele Frequencies obtained from gnoMAD v2.1 (https://gnomad.broadinstitute.org/

).

Table 2. *SRC-1* variant carriers included in clinical studies.

Study	SRC-1 variant	Age (years)	Sex (M/F)	BMI (kg/m^2)	BMI SDS
Core Phenotyping	Q463H*	18.2	F	42.1	
Core Phenotyping	Q463H	44.2	M	31.7	
Core Phenotyping	N549S	36.8	F	28.7	
Core Phenotyping	Q597P	47.4	M	35.1	
Core Phenotyping	Q597P	29.4	F	32.9	
Core Phenotyping	Q597P	28.1	M	40.0	
Core Phenotyping	Q597P	25.1	M	33.8	
Core Phenotyping	Q597P	20.9	M	24.8	
Core Phenotyping	S603C	33.0	M	44.5	
Core Phenotyping	A857T	28.2	F	35.5	
Core Phenotyping	T979P*	19.3	F	40.8	
Core Phenotyping	T979P	47.9	M	31.2	
Core Phenotyping	T979P	22.0	F	27.0	
Core Phenotyping	L1376P	48.0	F	37.5	
Core & Metabolic	T377N*	20.6	F	50.6	
Core & Metabolic	M381R*	28.0	F	53.1	
Core & Metabolic	H431R*	23.1	F	50.9	
Core & Metabolic	R572S*	24.1	M	52.7	

Core & Metabolic	R572S	49.8	F	48.3	
Core & Metabolic	D710H	47.6	F	50.6	
Core & Metabolic	A715T	39.0	F	33.3	
Core & Metabolic	A857T*	29.6	F	57.5	
Core & Metabolic	A857T*	32.6	M	74.8	
Core & Metabolic	P1034L	40.0	F	31.8	
Core & Metabolic	Q1231E*	18.7	M	55.6	
Core & Metabolic	Y1277C*	18.3	M	38.5	
Core & Metabolic	N1332S	18.9	M	23.3	
Core & Metabolic	N1332S	40.6	M	29.7	
Core & Metabolic	L1376P*	20.4	F	50.5	
Paediatric	T377N	12.6	M	29.3	2.1
Paediatric	T377N *	14.1	F	46.3	4.1
Paediatric	T377N*	13.3	F	41.1	2.8
Paediatric	T377N	13.3	F	32.9	2.4
Paediatric	H431R*	16.0	F	52.3	4.4
Paediatric	N549S*	13.0	M	35.1	3.3
Paediatric	Q597P*	17.0	M	32.3	2.7
Paediatric	S603C*	10.0	F	32.8	3.5
Paediatric	S603C	9.0	M	30.3	3.5
Paediatric	D710H	5.9	M	16.8	1.0
Paediatric	D710H*	9.9	M	27.9	2.2
Paediatric	D710H	11.8	M	18.5	0.2
Paediatric	A715T*	13.0	F	41.2	3.8
Paediatric	A715T	16.0	M	-	-
Paediatric	P1034L*	10.0	F	35.6	3.6

Paediatric	N1212K*	16.0	F	36.8	2.2
Paediatric	N1332S*	9.5	M	33.6	2.7
Paediatric	N1332S	13.5	M	25.9	1.7

Forty-seven *SRC-1* variant carriers (22 probands (indicated*), 25 family members) consented to participate in physiological studies. All 29 adults participated in a core phenotyping protocol; a subset of 15 adults participated in metabolic studies. Eighteen children were studied on a limited paediatric protocol. Abbreviations: BMI, body mass index; SDS, standard deviation score; F, female, M, male (- indicates information not available).

Table 3. Metabolic and endocrine measurements in adult *SRC-1* variant carriers compared to age, sex and BMI matched controls.

	Reference Range	**SRC-1 CASES**	**CONTROLS**
		n=29	n=30
% Male		45	50
Endocrine			
TSH, mU/L	*0.35 – 5.5*	1.9 ± 0.2	2.2 ± 0.2
Free T4, pmol/L	*10.0 – 19.8*	14.5 ± 0.3	14.4 ± 0.3
Free T3, pmol/L	*3.5 – 6.5*	5.1 ± 0.1	5.1 ± 0.1
Oral glucose tolerance test (OGTT)			
Fasting glucose, mmol/L	*3.5 – 5.5*	4.6 ± 0.1	4.8 ± 0.1
Fasting insulin, pmol/L	*0 - 60*	123.8 ± 16.1	110.0 ± 8.4
AUC glucose (mmol min/L)		1126 ± 70	1203 ± 96
AUC insulin (pmol min/L)		2062 ± 414	1535 ± 314
Lipids and liver function tests			
Total cholesterol, mmol/L	*0.0 – 5.2*	4.7 ± 0.2	4.4 ± 0.1
Calculated LDL cholesterol, mmol/L	0.0 – 2.6	2.9 ± 0.2	2.8 ± 0.1
HDL cholesterol, mmol/L	*1.0 – 1.5*	1.2 ± 0.06	1.0 ± 0.04
Triglycerides, mmol/L	*0.0 – 1.68*	1.5 ± 0.1	1.5 ± 0.1

Albumin, g/L	*35 - 52*	37.2 ± 0.5	36.2 ± 0.6
ALT, U/L	*10 - 49*	29.3 ± 2.4	34.7 ± 2.7
ALP, U/L	*53 - 129*	77.7 ± 3.7	77.2 ± 4.9
Bilirubin, µmol/L	*0 - 20*	10.4 ± 1.1	11.4 ± 1.3
De novo lipogenesis (DNL)~			
Fasting DNL, %		6.8 ± 0.9	7.0 ± 0.7
Fasting DNL, µmol/L		104.8 ± 20.9	89.2 ± 14.9
Post prandial DNL, %		12.3 ± 0.8	13.4 ± 1.5
Post prandial DNL, µmol/L		292.7 ± 45.8	283.2 ± 54.9
Fasting 3-hydroxybutyrate, µmol/L		67.5 ± 12.9	50.4 ± 10.0
Post prandial 3-hydroxybutyrate, µmol/L		27.9 ± 8.5	15.1 ± 2.1
Fasting NEFAs, µmol/L		517.4 ± 39.6	512.2 ± 36.8
Post prandial NEFAs, µmol/L		191.7 ± 15.6*	137.1 ± 18.7
Heart rate (HR) variability and BP			
Mean HR awake, bpm		66 ± 1.8	68 ± 1.9
RMSSD awake, ms		61.3 ± 9.0	50.5 ± 7.4
HF awake, ms^2		2010 ± 803	1521 ± 464
LF awake, ms^2		2800 ± 1292	1109 ± 179
LH/ HF ratio awake		2.5 ± 0.8	2.5 ± 0.5
Mean HR overnight, bpm		68 ± 2.1	68 ± 1.8
RMSSD overnight, ms		59.5 ± 7.2	54.9 ± 7.2
HF overnight, ms^2		1799 ± 441	1369 ± 388
LF overnight, ms^2		1502 ± 400	1638 ± 318
LH/ HF ratio overnight		1.5 ± 0.3	3.0 ± 0.7
SBP, mm Hg	*90 - 140*	125 ± 3	127 ± 3

DBP, mm Hg	*60 - 90*	75.9 ± 2.2	75.7 ± 2.0

Values are presented as mean ± standard error of the mean. *p<0.05, otherwise there was no significant difference between cases and controls. Abbreviations: ALP, alkaline phosphatase; ALT, alanine aminotransferase; AUC, area under the curve; BP, blood pressure; DBP, diastolic blood pressure; DNL, *de novo* lipogenesis; HDL, high density lipoprotein; HF, high frequency; HR, heart rate; LDL, low density lipoprotein; LF, low frequency; NEFA, non-esterified fatty acid; ns, not statistically significant; RMSSD, root mean square of successive differences; SBP, systolic blood pressure; TSH, Thyroid-Stimulating Hormone; ~ a subset of people underwent detailed metabolic phenotyping (Table 2).

Figure 1

(a)

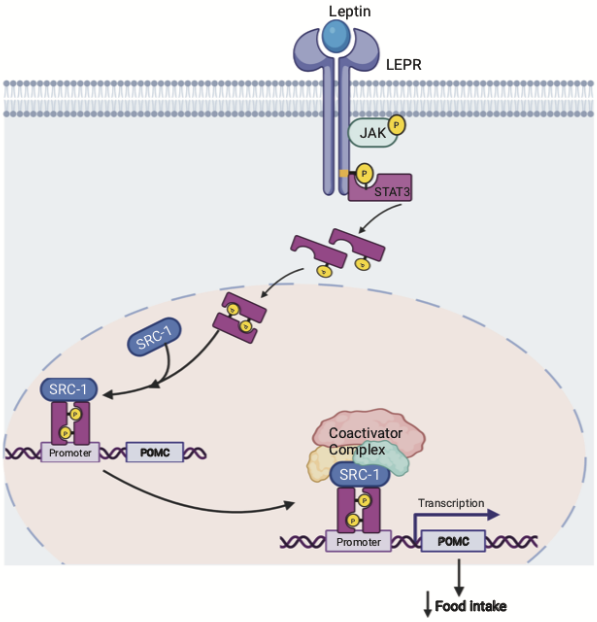

(b)

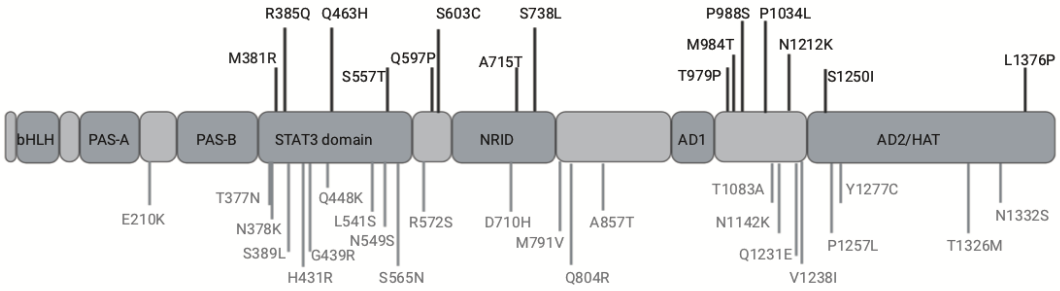

FIGURE 2

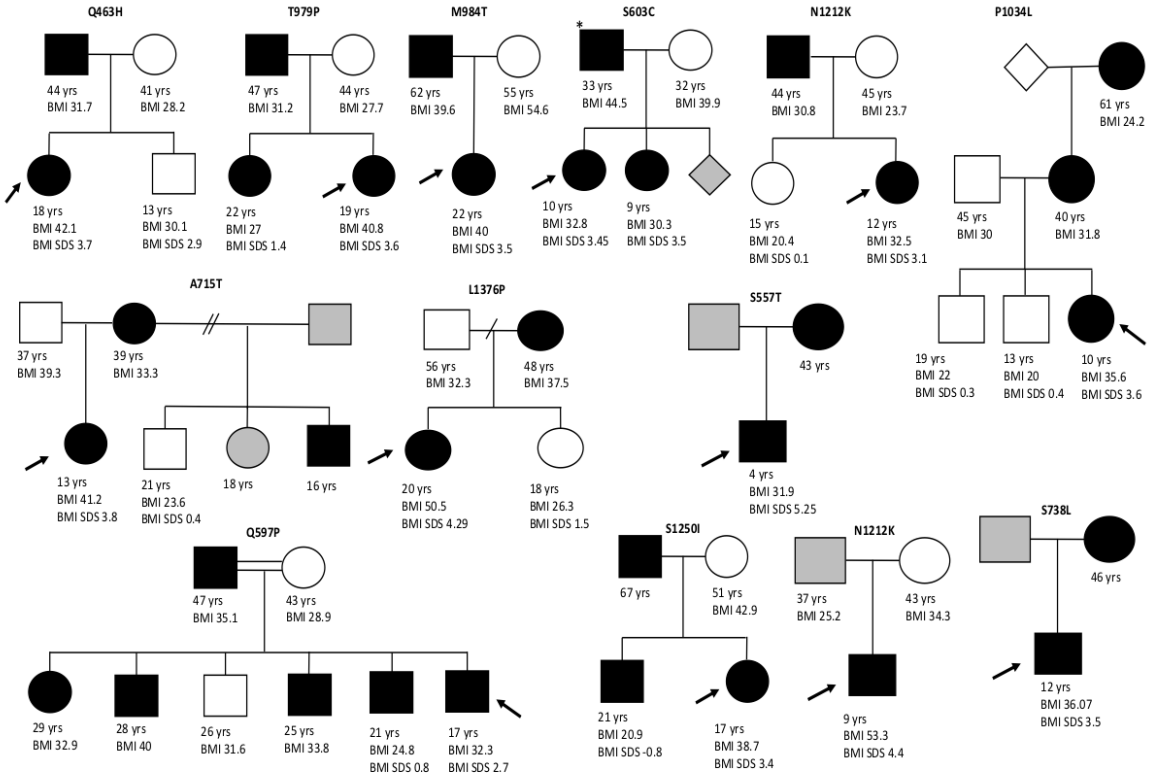

FIGURE 3

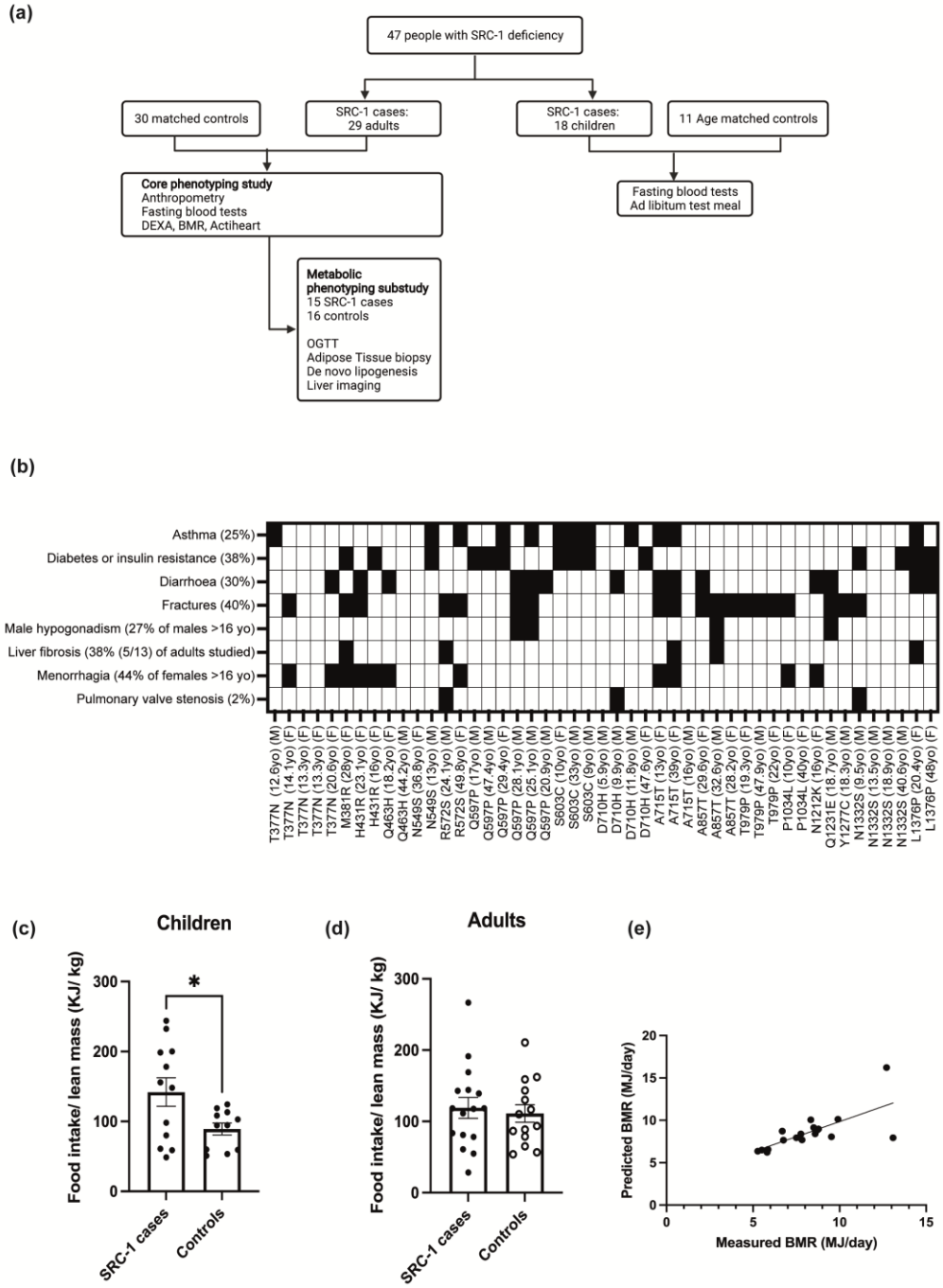

FIGURE 4